

**UNCLASSIFIED**

---

---

**AD 253 541**

*Reproduced  
by the*

**ARMED SERVICES TECHNICAL INFORMATION AGENCY  
ARLINGTON HALL STATION  
ARLINGTON 12, VIRGINIA**



---

---

**UNCLASSIFIED**

NOTICE: When government or other drawings, specifications or other data are used for any purpose other than in connection with a definitely related government procurement operation, the U. S. Government thereby incurs no responsibility, nor any obligation whatsoever; and the fact that the Government may have formulated, furnished, or in any way supplied the said drawings, specifications, or other data is not to be regarded by implication or otherwise as in any manner licensing the holder or any other person or corporation, or conveying any rights or permission to manufacture, use or sell any patented invention that may in any way be related thereto.

151 300

CATALOGED BY ASTIA  
S AD NO. 253541

61-2-6  
XEROX

CHARACTERIZATION OF SQUIB MK 1 MOD 0  
Capacitor Discharge Sensitivity Instrumentation (U)

10 JANUARY 1961



- RELEASED TO ASTIA  
BY THE NAVAL ORDNANCE LABORATORY
- Without restrictions
  - For Release to Military and Government Agencies Only.
  - Approval by BuWeps required for release to contractors.
  - Approval by BuWeps required for all subsequent release.

U. S. NAVAL ORDNANCE LABORATORY

WHITE OAK, MARYLAND

625200

ASTIA  
RECEIVED  
APR 6 1961  
JIPDR

CHARACTERIZATION OF SQUIB MK 1 MOD 0  
Capacitor Discharge Sensitivity  
Instrumentation

Prepared by:  
J. N. Ayres

Approved by:



Chief, Explosion Dynamics Division

ABSTRACT: Instruments and techniques have been developed to determine the statistical distribution function for the sensitivity of EEDs such as the Squib Mk 1 when fired by the capacitor discharge method. The design of the system has been oriented toward minimum distributed resistance and capacity without excessive distributed inductance. The control of input energy is better than  $\pm 0.5\%$ . The upper and lower limits of energy transfer have been determined for various input energies and are presented in equation and in tabular form. Monitoring, by cathode ray oscillography and with an ergmeter, permitted the measurement of the firing system efficiency and the detection of switching anomalies, which, in turn permitted the correction and censoring of data.

PUBLISHED MARCH 1961

Explosions Research Department  
U. S. NAVAL ORDNANCE LABORATORY  
WHITE OAK, MARYLAND

NavWeps Report 7308

10 January 1961

The work reported herein has been carried out as a part of the Naval Ordnance Laboratory's participation in the HERO (Hazards of Electromagnetic Radiation to Ordnance) Program, Task NOL-443. The objective of the HERO effort at NOL is generally to characterize the response of electro-explosive devices to electrical energy. This report describes the apparatus and calibration techniques applicable to the measurement of the initiation sensitivity of electro-explosive devices to capacitor discharge pulses.

This work should be of interest not only to the HERO project but also to the broad field of electro-explosive device design, development, manufacture, test, and use.

W. D. COLEMAN  
Captain, USN  
Commander

  
C. J. ARONSON  
By direction

## CONTENTS

	Page
Introduction . . . . .	1
Instrumentation . . . . .	3
Experimental Procedure . . . . .	16
Evaluation, Conclusions . . . . .	26
Appendix I: Estimation of Firing System Reliability Requirement . . . . .	27
Appendix II: Principles of the Bolometer-Ergmeter. . .	28

## ILLUSTRATIONS

Table 1: Typical Firing Signals . . . . .	2
Table 2: Energies Delivered by 4.00 Microfarad Capacitor Serial No. VQ 40 as a Function of Charge Potential . . . . .	21
Table 3: Delivered Energies (Not Corrected for Diode Errors) for Various Capacitors . . . . .	24
Figure 1: Elements of CD Firing Set . . . . .	4
Figure 2: Circuit Analysis of a CD Firing Set . . .	4
Figure 3: Photograph of CD Apparatus . . . . .	8
Figure 4: CD Firing System . . . . .	9
Figure 5: Plug-In Capacitor . . . . .	11
Figure 6: Firing Switch Capsule . . . . .	11
Figure 7: Details of Firing Chamber and Interlock. .	13
Figure 8: Design of 100/1 Attenuator for Ergmeter. .	15
Figure 9: Typical CD Oscillograms . . . . .	17
Figure 10: CD Transfer of Capacitor Serial Number VQ 40 . . . . .	19
Figure 11: Dielectric Leakage Resistance Measurement.	24
Figure II-1. Bolometer-Wheatstone Bridge . . . . .	29
Figure II-2. Bolometer Time-Temperature Excursion . .	30
Figure II-3. Symbolic Representation of Ergmeter . .	31
Figure II-4. Ergmeter Wiring Diagram . . . . .	33
Figure II-5. Ergmeter Polarizing Potentials . . . . .	35
Figure II-6. Contact Potential Diode Error . . . . .	37
Figure II-7. Total Diode Error . . . . .	37

Note: Although the names of commercial products are mentioned, no endorsement nor criticism of these products by the Naval Ordnance Laboratory is implied.

CHARACTERIZATION OF SQUIB MK 1 MOD 0  
Capacitor Discharge Sensitivity  
Instrumentation

INTRODUCTION

1. One of the phases of the HERO\* program at the Naval Ordnance Laboratory includes a detailed study of the firing response of a typical wire bridge (EED, Electro-Explosive Device) to electrical initiating energy. This study was intended to give information to serve as a design basis for development of an EED simulator — a non-explosive device having as near as possible the same electro-thermal properties as an EED, but equipped with a transducer to measure nondestructively power levels being delivered to the EED bridge wire. The study was also intended to give a better understanding of the way an EED converts electrical energy into explosive response. Such knowledge would be expected to aid in the creating of EEDs inherently less susceptible to EMR (Electromagnetic Radiation). Such knowledge should also be of benefit in improving coordination of the design of EEDs with their corresponding firing circuitry.

2. An essential part of the characterization of an EED is the measurement of its sensitivity parameters — how the EED will respond to various electrical pulses. There are a number of firing sources which could be used in laboratory firing and which represent to various extents the electrical environment possibilities in service. See Table 1.

3. The EED firing response depends on the wave form, power, and energy of the firing pulse. This response may be described as a statistical distribution function dependent upon the specific pulse being studied.

-----  
\* HERO - Hazards of Electromagnetic Radiation to Ordnance:  
A joint services program to detect, evaluate, and  
protect against circumstances wherein radio and radar  
can interfere with ordnance or ordnance systems.

Table 1: Typical Firing Signals

<u>Designation</u>	<u>Source Impedance</u>	<u>Typical Source</u>	<u>Remarks</u>
Capacitor Discharge	Low	Charged Capacitor	none
Constant Current	High	Electron Tube	Either steady-state or pulsed DC; Either steady state or pulsed RF assuming RMS current level is constant
Constant Voltage	Low	Battery	Most apt to be steady state or pulsed (switched) DC
Constant Power	Same as EED	Matched RF Transmission Line	Often encountered as a practical condition between constant current and constant voltage. Sometimes intentionally designed for.

4. In the past the distribution function generally used for expressing stimulus-response relationships has been chosen on the basis of trial-and-error experience and judgment but has not been investigated by extensive experimentation. Such experimentation would require a very large sample size — 5,000 or more units. Fortunately two lots of Squibs Mk 1, each of 10,000 units, were made available for the characterization program permitting the firings necessary to determine the distribution function (statistical model) of the EED sensitivity.

5. It was decided that the CD (Capacitor Discharge) firing technique would be used to investigate the following factors:

- (a) The statistical model for the sensitivity of the Squib Mk 1.
- (b) The agreement between the model and estimates based on normal sample size.

- (c) The reliability of the Squib Mk 1.
- (d) The effect of capacitor size on the CD sensitivity of the Squib Mk 1.
- (e) The CD sensitivity of the Squib Mk 1 in multiple combinations.

6. This report is written to present the instrumentation theory, design considerations, and evaluation associated with this program.

#### INSTRUMENTATION

7. Circuit Concept. On the surface, CD firing appears to offer a simple method for applying quantitative energy pulses to an EED. As can be seen in Figure 1, the basic circuit elements are:

- a capacitor
- a power supply to provide a charging potential
- a means for:
  - storing charge on the capacitor,
  - dumping the stored energy into the EED.

8. Practical Circuit Limitations. Figure 1 presents an over-simplified picture of life in the testing laboratory. Because of less than ideal qualities of the components and because of distributed electrical circuit parameters, the energy stored in the capacitor is not all delivered to the EED. Great care must be used to assemble the instrumentation from the best available material and to assess the efficiency of the assembly. Figure 2 is a portrayal of some of the circuit deviations from ideal.

9. The firing capacitor is different from the ideal in a number of ways. The charge is stored on metal foils of large surface area. The removal or introduction of charge is accomplished by using the foils as the conductors leading to the terminals. Ordinarily the cross sectional area of the foils presented to the electron flow is much greater than the terminal cross sectional area. The resistance to electron flow is therefore usually encountered in the capacitor leads and lead-to-foil connections. This "surge" resistance, plus the series resistance of all of the conductors and connectors, plus the series resistance within the firing switch have been lumped together into  $R_s$ .

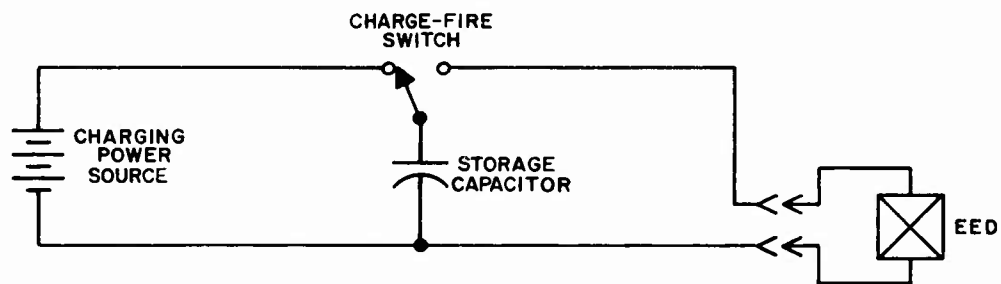


FIG. 1 ELEMENTS OF CD FIRING SET

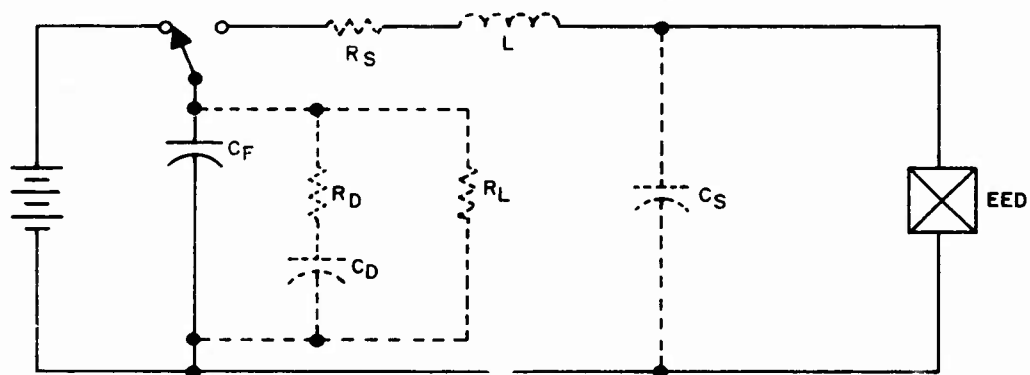


FIG. 2 CIRCUIT ANALYSIS OF A CD FIRING SET

10. Two other frailties of capacitors have been represented by  $R_L$  (the leakage resistance) and by the combination  $R_D, C_D$  (dielectric absorption).  $R_L$  represents the fact that insulators are less than perfect. Dielectric absorption is a term used to classify the behavior of a dielectric which, because of the molecular rearrangement attending a storage or removal of a charge, takes a finite time for completion and appears to hold back a part of the stored energy even when the capacitor is shorted out. This "held-back" stored energy (residual charge) is then released at a slower rate over a longer time with a pseudo time constant  $R_D \cdot C_D$ .

11. It is not possible to build a practical circuit whose inductance is non-existent, although the actual inductance may be and often is negligible. The necessity for inclusion of circuit interlock and safety enclosures for the EED introduces extra wiring and therefore extra inductance. This inductance has been lumped with the series inductances of the capacitor, firing switch, and EED in the term  $L$ .

12. The distributed capacity of the circuit into which the energy is dumped is represented by  $C_S$ . This circuit consists of the normally open contact of the firing switch, the leads to the firing chamber, the interlocks, and the EED leg wires.

13. The circuit transfer efficiency (the ratio of delivered energy to stored energy) will be less than 1.0. As a working model of the behavior of such a circuit the following equation is useful:

$$D = KS - L$$

where  $D$  is delivered energy (millijoules)

$K$  is a loss ratio

$S$  is stored energy (millijoules)

$L$  is offset loss (millijoules).

$L$  is considered to be a correction factor to take into account losses independent of the size of the stored energy. Such losses could be expected within a switch at the time of transition to a conduction state. Both  $K$  and  $L$  are correction factors determined empirically.  $K$  is to a fair degree subject to analysis and interpretation.

14. It is easy to show the effects of the distributed resistance and capacity, and also of the absorption capacity, provided  $R_D \cdot C_D$  is large compared to the discharge time constant:

$$K = M \frac{R_{EED}}{R_{EED} + R_S} \cdot \frac{C_F}{C_F + C_S} \cdot \frac{C_F}{C_T}$$

where  $R_{EED}$  = resistance of the EED

$$C_T = C_F + C_D$$

M is used to compensate for what we can't understand.

Whether  $C_T$  or  $C_F$  is known for a specific capacitor depends upon the capacitor measurement technique. For a Squib Mk 1 (whose resistance is about 1 ohm) a distributed resistance of 0.1 ohm could cause a 10% reduction in transfer efficiency. Great care must be exercised to attain  $R_S$  values of 0.2 ohm or less. With firing capacitors above 0.1 microfarad the losses due to  $C_S$  should be readily controllable. Dielectric absorption losses are controlled by the choice of capacitor. Apparently Mylar dielectric or polystyrene dielectric capacitors are the most suitable and can be had with less than 1% dielectric absorption.

15. Dielectric leakage ( $R_L$ ) can affect the amount of energy available for delivery to the EED only if the switching time (transfer time between "charge" and "fire") is greater than 1% of the leakage time constant,  $C_F \cdot R_L$ . Fortunately many of the capacitors which have low dielectric absorption also can be expected to have large leakage time constants — 10 or 20 hours or more.

16. The distributed inductance can be expected to introduce wave form distortion. An excessive amount of inductance would be expected to give rise to an underdamped oscillation. It is believed that a somewhat overdamped or critically damped R-C discharge represents the best practical wave form for capacitor discharge firing. A pure R-C wave form (negligible inductance) could be expected to lose energy by electromagnetic radiation in the higher frequencies necessary to transmit the pulse. Also, the peak current levels could be expected to emphasize nonlinearities in the circuit parameters. A highly underdamped discharge could markedly increase the power dissipation time constant over the theoretical R-C time.

17. Reliability Requirements. In the practical testing system it is necessary to be able to set the energy level (intensity of stimulus) by being able to control the charging potential and capacitor size, and by being able to measure the transfer efficiency. Perhaps somewhat less obvious is the necessity for having a reliable, as well as an accurate, firing system. At a given test level, an observed reliability can be accepted as being a property of the EED only if the observed failure rate cannot be attributed to partial or complete switch failure, low potential, bypassing of EED, etc. It was in the original plan of the investigation to determine by experiment the statistical distribution function of the Squib Mk 1 using the Bartlett Plan for assigning samples to the test conditions. This plan entails the testing of a large number of samples (over 7,000 in the present instance) mostly at very high and very low functioning levels. All possible care had therefore to be exercised in the experimental procedures.

18. As an example, during the Bartlett Test, 2,486 Squibs Mk 1 were pulsed with a 4-microfarad capacitor charged to 33.59 volts. All fired except two. Were these two failures due to the fact that the firing energy was at or near the 99.9195% functioning point? Was it because the firing apparatus was only 99.9195% reliable? Was it a combination of a somewhat higher functioning level than 99.9195% and a somewhat more reliable switch than 99.9195%? If the firing system reliability was 99.9195% or higher, then in this case we would be able to say with 95% confidence that the observed two failures in 2,486 is a property of the EED (See Appendix I).

19. Experimental Set-up. The instrumentation assembled for the CD firing, Figure 3, is represented schematically in Figure 4.

20. A massive copper bus-bar system was constructed with the design emphasis towards high circuit conductivity, high insulation resistance, low distributed capacity, and good dimensional stability. The final design was accomplished with some slight sacrifice of low distributed circuit inductance. This inductance was, however, not large enough to cause undesirable distortion of the pulse wave forms required for the experimental program. A plug-in capacitor system was used to facilitate capacitor size changes.

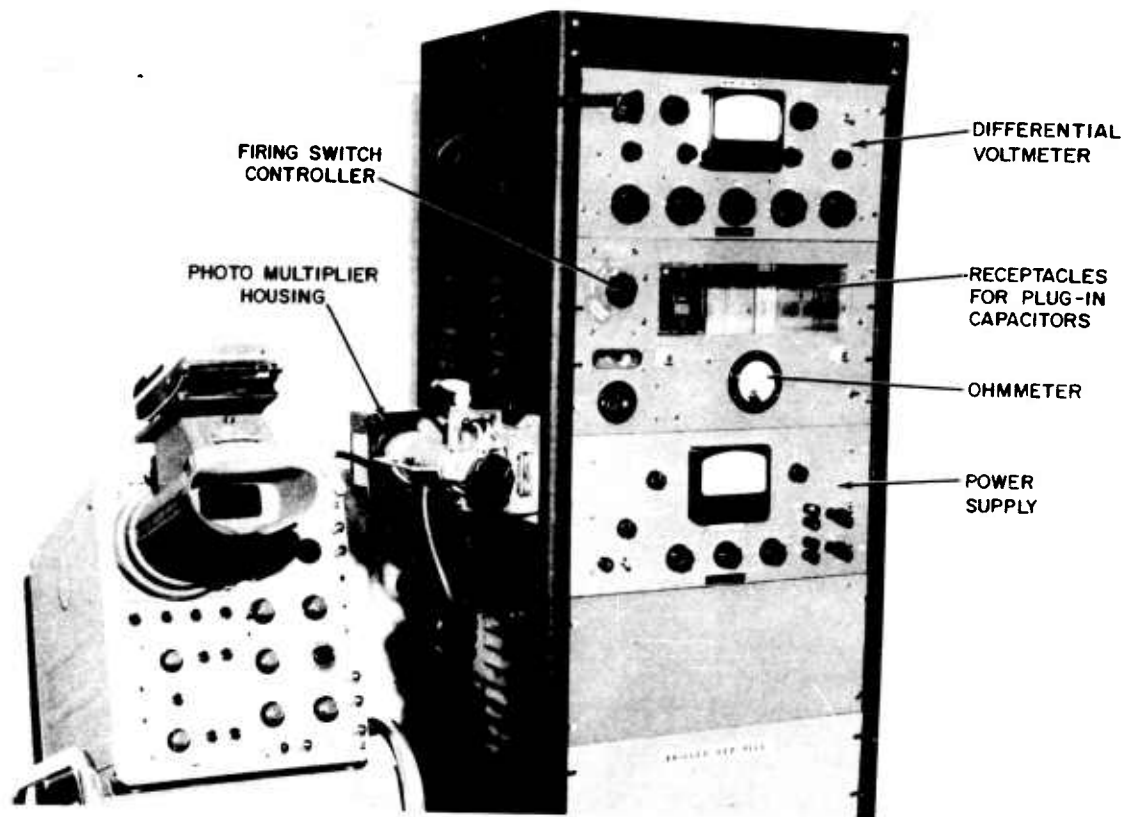


FIG. 3 PHOTOGRAPH OF CD APPARATUS

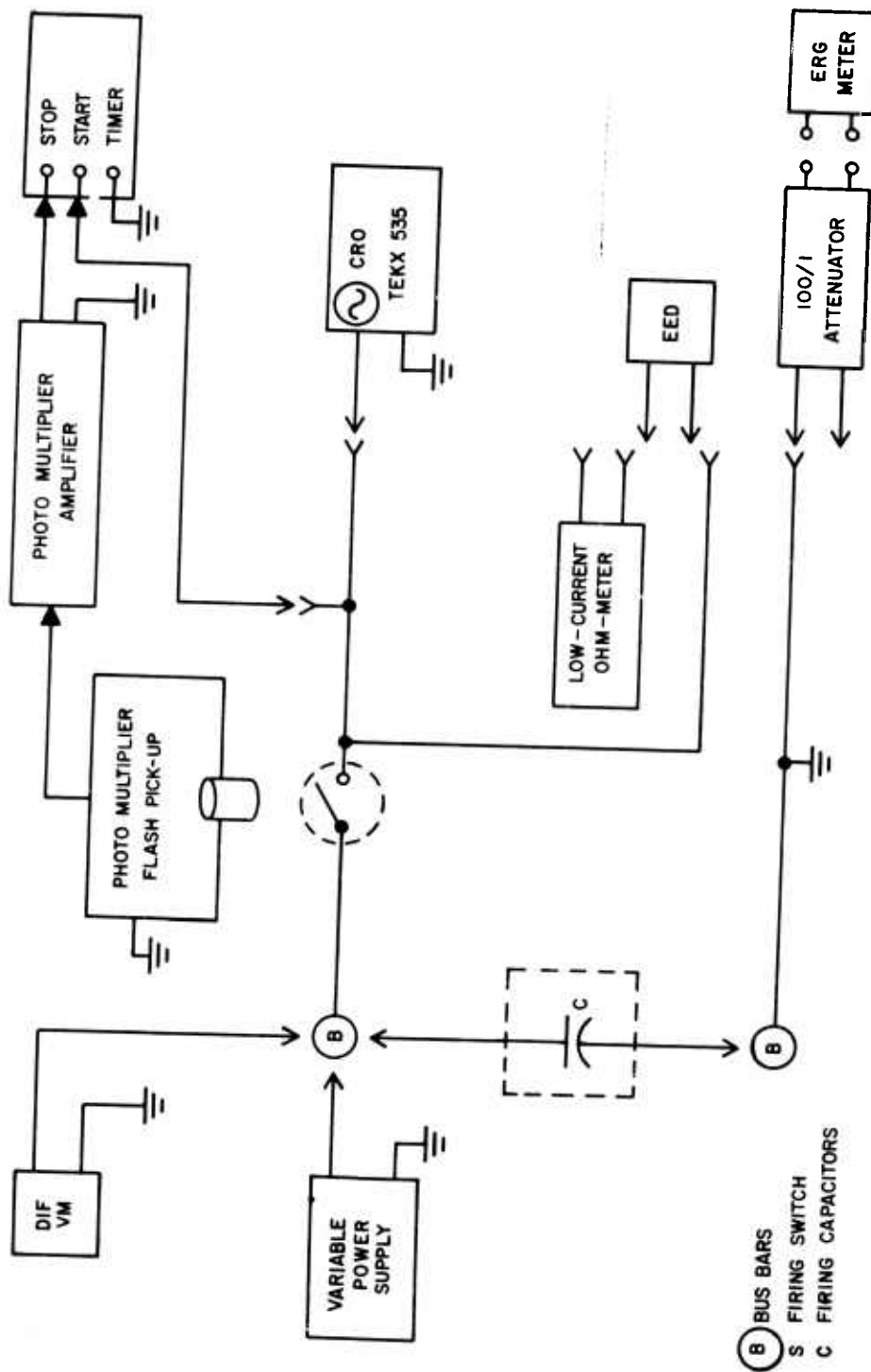


FIG. 4 CD FIRING SYSTEM

B BUS BARS  
 S FIRING SWITCH  
 C FIRING CAPACITORS

21. The capacitor plug-in connectors (see Figure 5) were designed to have multiple spring-loaded, sharp-edged line contacts giving reproducibly low contact resistance (below 1 milliohm). The capacities of the plug-in capacitors were determined to better than 0.2%. No capacitors were employed whose leakage time constants\* were less than 20 minutes.

22. The capacitor charging potential was maintained by a John Fluke Type 407 precision power supply and monitored by a John Fluke Type 801 differential voltmeter. The regulation and accuracy of the system is believed to be better than 0.1% in the range of 1 to 400 volts. The John Fluke Type 301E precision DC supply is an example of a single instrument, now available, which could be used to perform the function of the power supply and differential voltmeter just mentioned.

23. All CD firing pulses were monitored with a CRO such as the Tektronix Type 535 or 545 and recorded photographically. The photographs were inspected for agreement between the observed peak pulse potential and the capacitor charge potential. The trace also was inspected for any wave form abnormalities such as might arise from switch malfunctioning.

24. The firing switch (Figure 6) is of the magnetic plunger evacuated, wetted-contrast, mercury, glass enclosed capsule type. Switching action was brought about by cam actuated permanent magnets. This type of switch is ordinarily, and more readily, operated by the solenoid action of a coil mounted coaxially with the switch capsule; but past experience had shown that solenoid energization and de-energization can cause transient currents in the EED circuit. Such transients, while not likely to cause EED initiation, are of sufficient magnitude to interfere with circuit calibration and monitoring.

-----  
\*For procedure for determination of leakage time constant see page 22, paragraph 39.

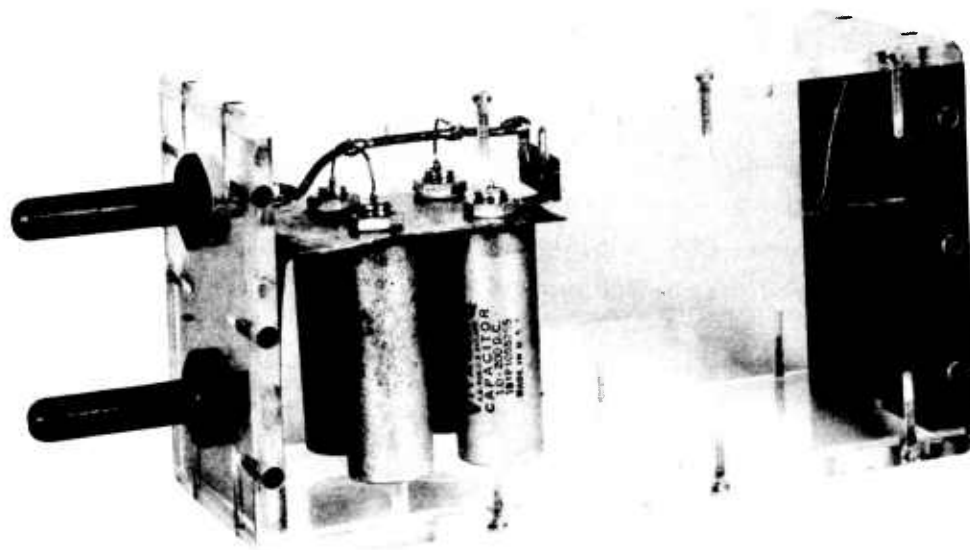


FIG. 5 PLUG-IN CAPACITOR

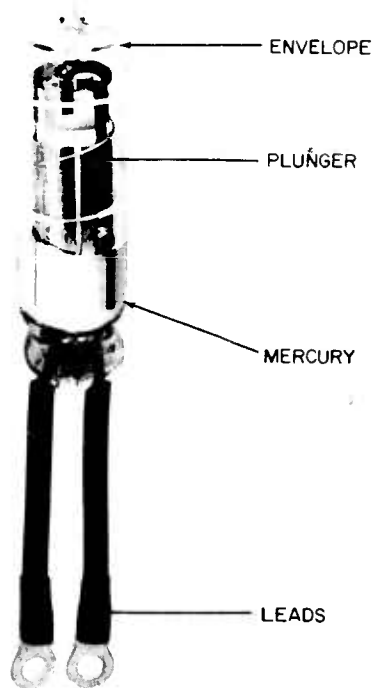


FIG. 6 FIRING SWITCH CAPSULE

25. In operation a rotating cam control mechanism programmed through the following steps:

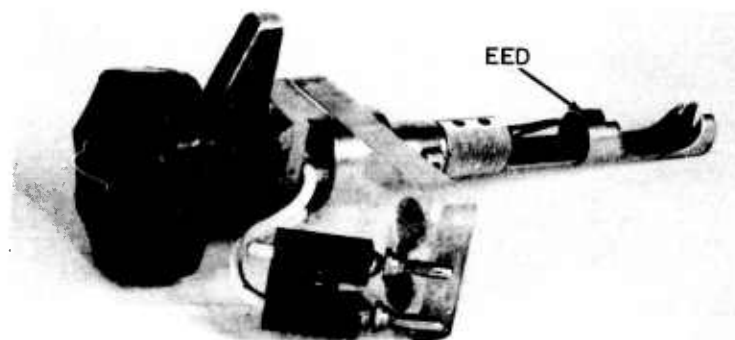
- (a) Measure EED resistance
- (b) Charge the capacitor and monitor charge potential
- (c) Disconnect the charging potential
- (d) Fire (trip permanent magnets)
- (e) Discharge residual charge on capacitor, short out EED receptacle.

The CRO and timer input circuits were left connected to the EED receptacle at all times because their input impedances were so high and input capacities so low that their effect on the firing circuit was negligible for firing capacities greater than 0.01 microfarad and discharge loads less than 1,000 ohms. By leaving them connected, the switching problem was considerably simplified.

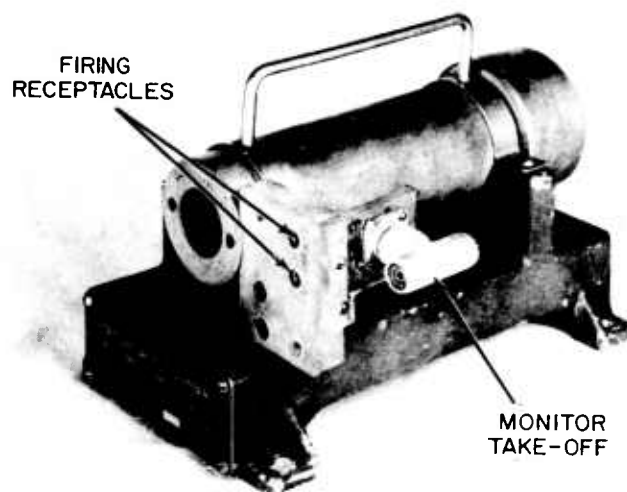
26. Firing was carried out in a modified Detonator Test Chamber Mk 3 Mod 0 (shown in Figure 7). The chamber was modified by the installation of a transparent end cover through which the output flash of the EED could be sensed by a photo-multiplier tube circuit for timing purposes. The micro-switch interlock disconnect was replaced by a high-current capacity, low resistance, direct action interlock. As is usually the case, a minor compromise had to be made in the interest of safety of operation. An extra circuit break and extra convolutions in the EED circuit had to be accepted in order to be able to provide mechanical protection to the operators. It is quite likely that some of the distributed resistance of the circuit can be attributed to the pressure contacts which were used to clamp the EED leg wires. However, the reduction in contact resistance that might be achieved by soldering the EED leg wires to the EED carrier was considered not to be warranted in the face of the extra work that would be involved in firing thousands of units. The detonator firing chamber was mounted physically as close as possible to the previously mentioned bus-bar system in order to keep total circuit dimensions to a minimum.

27. By a minor modification of the firing chamber, it was possible to install a photo multiplier circuit to sense the flash from the Squib Mk 1. A type 1P21 photo multiplier tube was chosen on the basis of maximum sensitivity commensurate with an adequate spectral response (out to 7,000 Å).

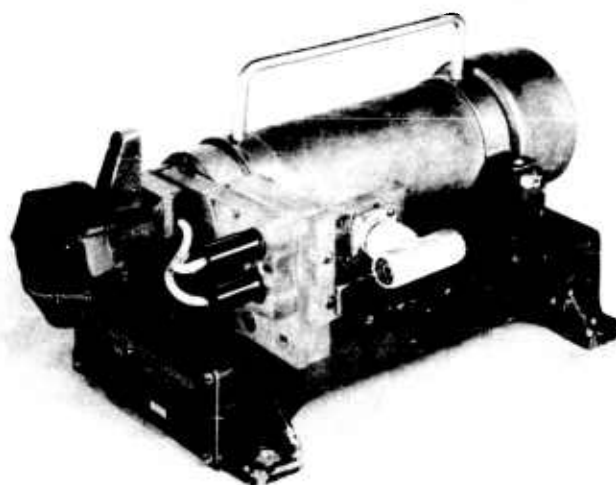
NAVWEPS 7308



EED CARRIER



FIRING CHAMBER



FIRING CHAMBER  
WITH EED CARRIER  
IN PLACE

FIG. 7 DETAILS OF FIRING CHAMBER AND INTERLOCK

The output of the photo multiplier was connected to an amplifier cathode follower circuit which drove the stop circuit of a Potter Model 471 eight-megacycle counter chronograph having a resolution of 0.625 microseconds. The timer was started by the leading edge of the capacitor discharge pulse. The timing system therefore measured the firing lag time of the EED — the time from initial application of firing energy to the time rupture of case and emission of "visible" radiation. Note that firing lag time is not the same as the initiation time of the EED since a finite time is required for build-up and propagation of sufficient chemical activity to bring about externally detectable explosive action.

28. Two alternative resistance measurement systems were available — one internally switched onto the bus-bar at appropriate times and one which was tied in at the monitor take-off. In addition to giving the somewhat academic information about the resistance distribution of the sample, bridge resistance data verify the quality of the contact between the EED and the EED carrier terminals and also the quality of the interlock contacts. By measuring the EED bridge resistance only after the EED (mounted on the EED carrier) was inserted into the firing chamber the "first rule" of EED testing safety was observed:

Never pass a current through an explosive loaded bridge wire unless the EED is sufficiently guarded to afford complete protection to the operator.

29. A Brunswick Instrument Co. Type 150 ergmeter (see Appendix II) was used to measure the transfer efficiency of the system. Measurement of the delivered energy by integration of the voltage wave form observed across the EED also requires a knowledge of either the resistance or the current wave form. As the bridge wire is heated to the firing point, the resistance changes appreciably (30 to 50% in the case of the Squib Mk 1). Determination of the resistance-time function could be made if the current-time function were known. The insertion of a current monitoring resistor in series with the EED can be expected to alter the discharge time constant and to divert part of the delivered energy from the EED. This is particularly true in the case of low resistance EEDs (like the Squib Mk 1) where a current monitoring resistor, whose resistance is large enough to make possible reasonably accurate measurements of the current wave form, will introduce time-constant and energy-partition errors.

Similarly, the ergmeter cannot be used during a firing by putting the ergmeter in series with the EED. Rather, it is used (on a substitution basis) before, after, and at intervals during a firing run in order to detect any deterioration in switch performance. The ergmeter can be adjusted to have a full scale sensitivity of 0.03 to 0.10 millijoules with an input resistance of 10 ohms.

30. A resistance network attenuator was devised (Figure 8) having a 1-ohm input (thus better simulating the conditions when firing the 1-ohm Squib Mk 1) and a 100/1 attenuation ratio. It is imperative that the attenuator introduce as little inductance into the circuit as possible in order to avoid disturbing the discharge wave form.

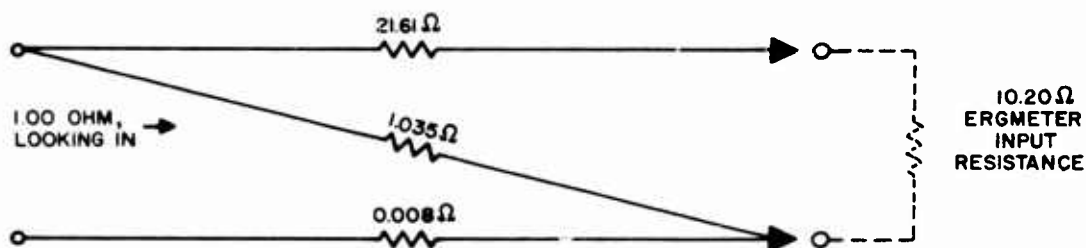


**FIG. 8 DESIGN OF 100/1 ATTENUATOR FOR ERGMETER**

It is also desirable to have the attenuator input connected as closely as possible to the point to which the EED is normally connected. The output end of the attenuator was required to be greater than 20 ohms for proper functioning of the ergmeter. It would have been desirable to have a 1-ohm input ergmeter system with a full scale sensitivity of 1.5 to 2.0 millijoules rather than 3.0 millijoules. This would either require an attenuator of considerably less than 100/1 attenuation (not compatible with the input-output resistance requirement) or an even more sensitive ergmeter (involving redesign of the instrument).

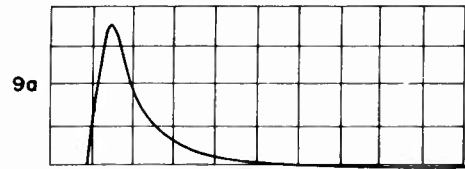
EXPERIMENTAL PROCEDURE

31. Switch Monitoring. At the outset of the program it was decided that oscillograms would be made of every CD shot by photographic recording of CRO traces. If any abnormal trace were observed or if a trace were not successfully recorded, that particular test shot was to be ignored (data discarded). Ergmeter readings were to be made at least at the beginning and the end of each day's firings. A shift in transfer efficiency (greater than that expected from experimental error) between consecutive calibrations would be the basis for rejecting all data obtained between the two calibrations. These precautions were taken to avoid false data that might derive either from occasional switch anomalies or from gradual switch deterioration. (See Figure 9.)

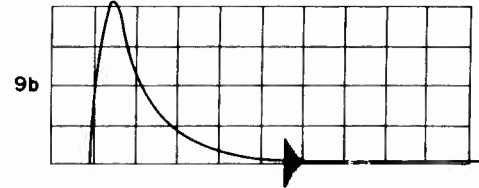
32. In the course of the firing program both forms of trouble were encountered. Early in the program some firings were carried out with small capacitors (0.3, 0.1 microfarad) with charge potentials in excess of 120 volts. Apparently the switch capsule was adversely affected by the high potentials (and high peak discharge currents). The switch capsule was replaced with the stipulation that charge potentials would not be allowed to exceed 70 volts.

33. Apparently cam-mechanism wear was a cause of erratic switch performance, (Figures 9 (e), (f), (g), and (h)) since such troubles were cured by mechanical changes (repositioning components, installing sponge rubber buffers, tightening clamps). Switch "bounce" was being caused by the impact of the magnets at the end of the trip stroke. A simple mechanical explanation is difficult to accept in view of the observed time interval (2 to 10 microseconds) between switch closure and "bounce". Such interval implies extremely rapid mechanical motions with a frequency range of 100 to 500 KC.

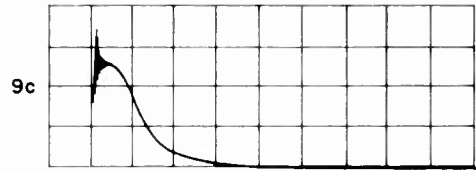
34. Even more difficult to understand is the voltage trace evidence that the capacitor appeared to regain potential during the "bounce" phase. This anomaly was evidence of a serious malfunction in that the delivered energy was found to be 50 to 80% of the norm whenever bounce was known to have occurred. In passing, it is of interest to note that whenever bounce was observed, the potential of the initial pulse peak was always abnormally low.



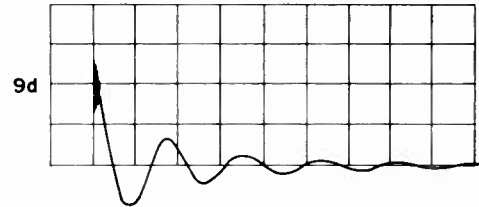
ACCEPTABLE TRACE



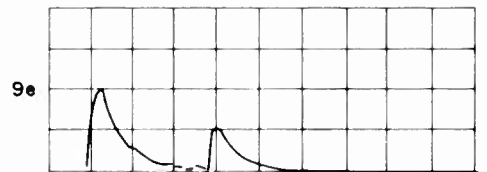
ACCEPTABLE TRACE, DISCONTINUITY  
AT POINT OF BRIDGE BURNOUT



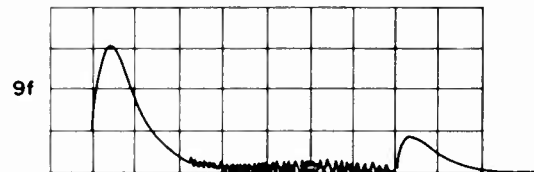
"RINGING" AT BEGINNING OF TRACE



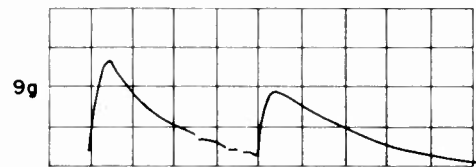
UNDERDAMPED RC DISCHARGE



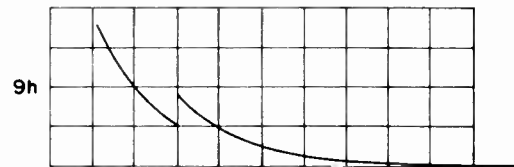
SWITCH "BOUNCE"



SWITCH "BOUNCE" PLUS "HASH"



SWITCH "BOUNCE" PLUS DISTORTION  
OF PULSE PEAK



SWITCH "BOUNCE" DURING MAIN  
DISCHARGE

FIG. 9 TYPICAL CD OSCILLOGRAMS

35. In addition to the detection of switch malfunctioning, the CRO monitoring also detected errors in setting of the charging potential as well as detecting wave form distortion such as that seen in Figures 9(c) and (d). With small firing capacitors (less than 0.3 microfarad) initial very high frequency oscillations were observed (Figure 9(c)). Such transients can be expected to dissipate energy by electromagnetic radiation. The trace observed in Figure 9(d) indicates that the inductance was unusually large, or the EED resistance, or the firing capacity was unusually low. Whenever anomalous behavior of any kind was observed, the data were discarded, and the trouble removed, usually by "symptomatic treatment". To search for the exact cause of the trouble was usually not warranted.

36. The particular ergmeter sensitivity settings that had to be used in the Squib Mk 1 testing program gave rise to a certain amount of jitter during half-sine wave burst calibrations. Furthermore the half-sine wave pulser could not be set sufficiently close to zero to permit a valid extrapolation to determine the "zero-offset" error (mentioned in Appendix II, paragraph 10). The contact potential error was determined to be 7 ergs (0.7 microjoule) referred to the input of the ergmeter. With a 100/1 attenuator this error would be 0.07 millijoule referred to the attenuator input connections.

37. As a standard, day-to-day procedure, the transfer efficiency was observed for the 4.00-microfarad firing capacitor, serial No. VQ 40, in the firing system shown in Figure 4 for stored energies of 1.0, 1.5, 2.0, 2.5, and 3.0 millijoules. Such observations were taken throughout the course of the program (nearly a year's time) and combined to give the best estimate of a straight line relationship between stored and delivered energy, curve  $\gamma$  of Figure 10. When the observed transfer efficiencies are corrected for the observed constant potential diode error then curve  $\beta$  of Figure 10 results. All calibrations of the ergmeter were performed by setting the ergmeter deflection at 80% of full scale with 0.025 millijoule half-sine wave input. With the 100/1 attenuator, this means that 2.4 millijoules of delivered energy should be equivalent to 80% of full scale deflection. The value of stored energy, picked off the best straight line fit of the data, corresponding to a delivered energy of 2.4 millijoules, was a direct measure of the transfer efficiency of the CD apparatus. Zero offset errors are suppressed at this point since a substitution comparison is made between the half sine pulser and the CD apparatus under conditions of identical ergmeter deflection. If it is assumed

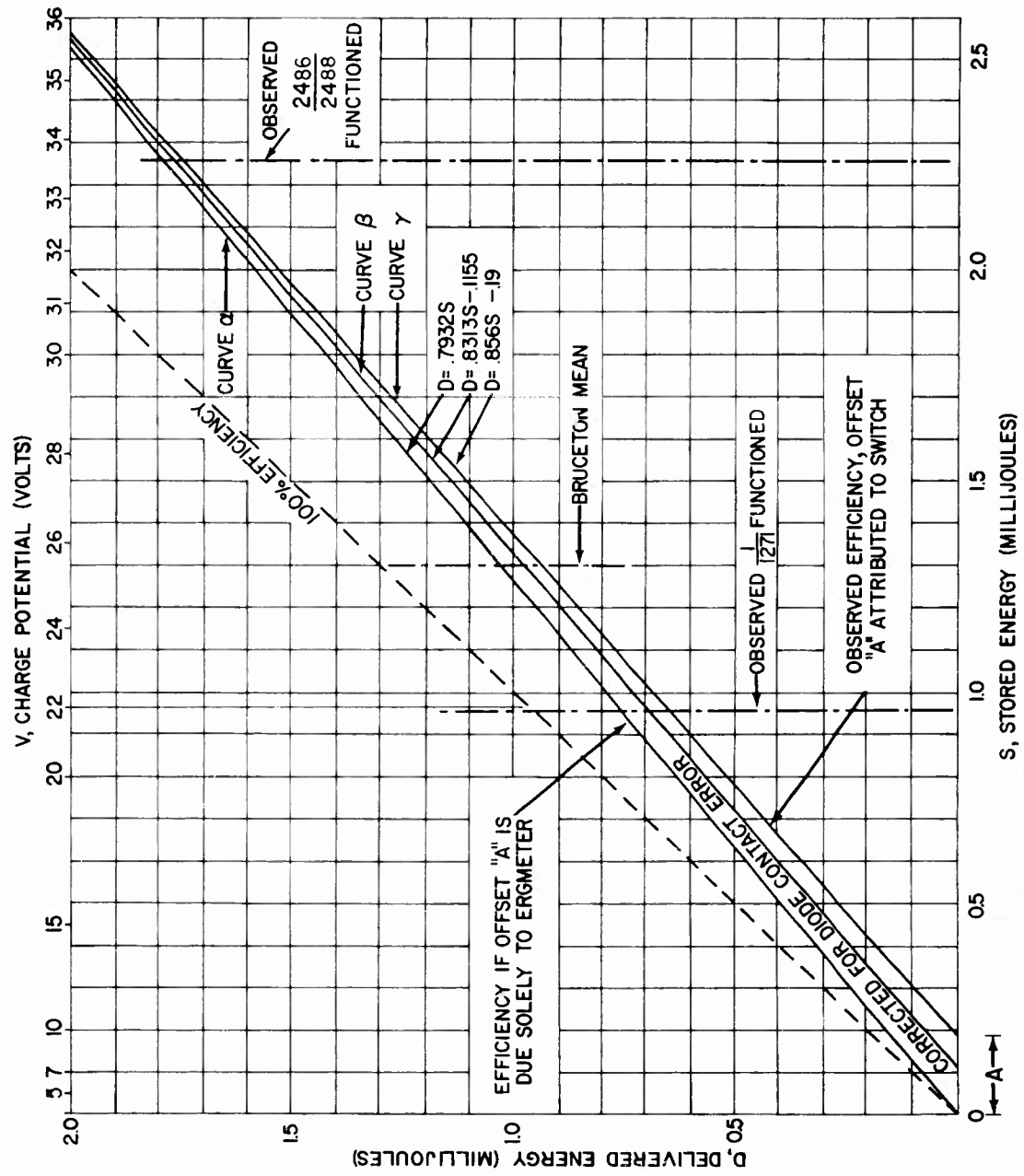


FIG. 10 CD TRANSFER OF CAPACITOR SERIAL NUMBER VQ 40

that the observed zero offset is due totally to diode error then the transfer efficiency observed at 2.4 millijoules delivered energy must also be the transfer efficiency at all other tested levels. Curve  $\alpha$  of Figure 10 expresses this relationship. The equations of these three curves are:

$$D_{\alpha} = 0.7932 S \quad (3)$$

$$D_{\beta} = 0.8313 S - .1155 \quad (4)$$

$$D_{\gamma} = 0.8560 S - .1900 \quad (5)$$

where S is the stored energy,

$D_{\alpha}$  is delivered energy assuming zero offset is due only to diode error

$D_{\beta}$  is delivered energy assuming zero offset not corrected for diode contact potential is switch error

$D_{\gamma}$  is delivered energy assuming zero offset is a property of the switch.

For some of the test levels used in various experimental program, the values of  $V_0$ , S,  $D_{\alpha}$ ,  $D_{\beta}$ , and  $D_{\gamma}$  are given in Table 2. Values of delivered energies can, of course, be computed for other levels of stored energy. It is believed that the true value of delivered energy falls between  $D_{\alpha}$  and  $D_{\beta}$ . Equation (4) could be interpreted as indicating that no delivered energy could be expected for stored energies of 0.1155 millijoule or less. It is difficult to accept that the CD apparatus loses 0.1155 millijoule before any energy is deliverable to the EED, since it is possible to deliver 0.02 millijoule at 80 to 90% efficiency into the un-attenuated 10-ohm input erg meter. At least part of the loss, however, could arise from nonlinearities in the switch and capacitor working into a 1-ohm lead. It is therefore believed that the  $D_{\alpha}$  equation is the most likely estimate; but that for safety considerations, the  $D_{\beta}$  is the more conservative estimate of the transfer efficiency of the system. On the basis of the  $D_{\alpha}$  equation it can be said that the value of the distributed series resistance,  $R_S$ , (see Figure 2) is 0.27 ohm .

Table 2: Energies Delivered by 4.00-Microfarad Capacitor  
Serial No. VQ 40 as a Function of Charge Potential

<u>V<sub>o</sub></u> <u>Volts</u>	<u>Energies (Millijoules)</u>			
	<u>S</u>	<u>D<sub>α</sub></u>	<u>D<sub>β</sub></u>	<u>D<sub>γ</sub></u>
33.59	2.257	1.790	1.760	1.742
32.87	2.161	1.714	1.681	1.660
32.16	2.069	1.641	1.604	1.581
31.48	1.982	1.572	1.532	1.507
30.81	1.899	1.506	1.463	1.436
30.17	1.820	1.444	1.398	1.368
29.53	1.744	1.383	1.334	1.303
28.92	1.673	1.327	1.275	1.242
28.32	1.604	1.212	1.218	1.183
27.74	1.539	1.221	1.164	1.127
27.15	1.474	1.169	1.110	1.074
26.62	1.417	1.124	1.063	1.023
26.08	1.360	1.079	1.014	0.974
25.56	1.307	1.037	0.971	0.929
25.06	1.256	0.996	0.929	0.885
24.57	1.207	0.957	0.888	0.843
24.09	1.161	0.921	0.849	0.804
23.62	1.116	0.885	0.812	0.766
23.17	1.074	0.852	0.777	0.729
22.74	1.034	0.820	0.744	0.695
22.31	0.996	0.790	0.712	0.662
21.90	0.959	0.761	0.682	0.631

38. Experience with capacitors from 0.3-microfarad capacity and up has shown no great anomalies or unexplainable results. Of course, none of the other capacitors has been tested to the degree that the 4.00-microfarad, serial no. VQ 40 capacitor has, this capacitor being the one used through the Bartlett determination of the statistical model of the Squib Mk 1. The value of  $R_S$  cannot be measured as precisely with a 10-ohm input system as it can be with the 1-ohm input. In general, however, the value of  $R_S$  for the various capacitors used in conjunction with the CD apparatus seems to lie in the region of 0.2 to 0.4 ohm, both for the 1- and 10-ohm inputs. Table 3 gives the observed transfer efficiencies of a number of different capacitors. The large capacitor sizes (above 90 microfarads) are made up of banks of 50-microfarad units in parallel. The 90-microfarad capacitor is a specially fabricated, pulse discharge service, Mylar dielectric capacitor and would be expected to exhibit maximum transfer efficiency. The 50-microfarad units are paper dielectric and not particularly good — in the order of 75% efficient. It is not reasonable to expect that paralleling such units would increase the efficiency. The results, then, at 190 microfarads and above are not reasonable and are considered to be due to the fact that the input signal time constant is too large for the ergmeter to accept without producing fictitious results (see Appendix II, paragraph 9).

39. Dielectric Leakage. Dielectric leakage can be measured quite simply by a technique such as is illustrated in Figure 11. The capacitor is connected to terminals A and B. Terminals B and C must be insulated from ground with a minimum leakage resistance of  $10^{14}$  ohms. The electrometer input resistance must be equally high. The capacitor is charged to potential  $V_1$  by shorting terminals C and D. Time is measured from the instant of removal of the C to D short to the time that the electrometer\* indicates a potential between C and D equal to  $0.01 \cdot V_2$ . From the properties of the exponential decay function, it can be shown that a decay of 1% will take place in 1% of the time constant. The leakage resistance will be given by:

$$R_L = \frac{100T_{1\%}}{C_1} \quad (6)$$

-----  
 \* The electrometer deflection results from the loss of the initial charge,  $C_1 \cdot V_1$ , on the capacitor because of the internal capacitor leakage.

where  $R_L$  is the leakage resistance,  
 $R_{1\%}$  is the time for a 1% loss in capacitor  
potential, and  
 $C_1$  is the capacitance.

40. Q-Meter Measurements. The distributed inductance, capacitance, and resistance of the CD apparatus can be measured by Q-meter techniques. The resistance will include dielectric losses of the circuit. It will not take into account dynamic resistive effects that would be associated with the closure of the switch. With the firing switch closed and by looking into the EED terminals with a Q-meter, measurements can be made under three conditions:

- (a) No capacitors plugged into the CD bus-bar system.
- (b) Dead short across the capacitor plug-in terminals (a short in place of the capacitor).
- (c) Capacitor plugged in in the standard fashion.

41. With no firing capacitor plugged into the CD bus-bar, the distributed capacity,  $C_S$ , can be measured. The effect of  $C_S$  is sensed by placing the test points across the Q-meter capacitor and by changing the setting of the Q-meter capacitor to restore the Q-meter to the original operating resonance frequency.

42. With a dead short substituted for the firing capacitor, the distributed resistance and inductance of the CD bus-bar system can be determined. This measurement is made by placing the circuit to be tested in series with the Q-meter inductor.

43. Additional inductance and resistance observed with the test capacitor plugged into the CD bus-bar in the normal manner is then a property of this test capacitor. The stray inductance and resistance measured by this arrangement and by the previous (shorted) arrangement should be lumped together in considering the complete system.

44. The Q-meter measurements should be made at a number of different frequencies. The inductance would be expected to be independent of frequency. As a consequence the reactance should increase linearly with frequency provided the stray capacity  $C_S$  is small enough to be ignored. The resistance versus frequency function should show the resistance independent of frequency until the capacitor of dielectric losses become significant, at which time the value of  $R_S$  should begin to increase.

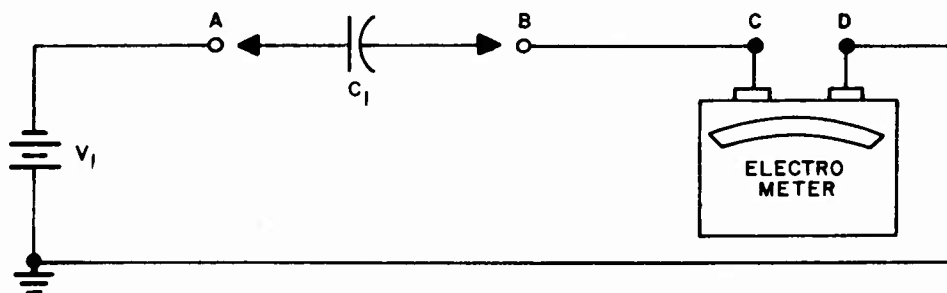


FIG. II DIELECTRIC LEAKAGE RESISTANCE MEASUREMENT

Table 3: Delivered Energies (Not Corrected for Diode Errors) for Various Capacitors

Capacitor Size (microfarads)	Serial Number	Charge Potential (volts)	Efficiency (%)
1.00	GR#1	77.46	77.7
4.00	VQ 40	38.73	79.3
7.00	VQ 23	29.28	79.6
10.00	VQ 42	24.50	79.5
21.0 (4 + 7 + 10)	VQ 40, VQ 23 VQ 42	16.90	82.0
48.5	F 42	11.12	75.5
90.0	NOL 6	8.17	87.3
188 (90 + 48.5 + 47.5)	NOL 6, F 42 F 15	5.65	97.2
49.5	F 21	11.01	72.5
48.5	F 40	11.12	69.0
48.6	F 37	11.11	74.5
48.7	F 34	11.10	69.5
195.3 (49.5 + 48.5 48.6 + 48.7)	F 21, F 40, F 37, F 34	5.54	96.5
1000	20 of the F-type capacitors	1.5 stored energy 1.125 milli- joules	256

NOTE: Except as noted, stored energy = 3.0 millijoules  
1-ohm input, 100/1 attenuator.

NavWeps Report 7308

45. Q-meter measurements:

(a) CD bus bar.  $C_S \approx 28$  to 33 micro microfarads.

Frequency (mc)	0.3	1.1	2.0	5.0
$R_S$ (ohms)	0.75	0.90	0.99	2.54
$X_S$ (ohms)	could	3.96	6.2	17.8
$L_S$ (microhenries)	not be resolved	0.64	0.81	0.7

(b) CD bus bar + 90 microfarad capacitor, NOL 6.

Frequency (mc)	0.1	0.3	1.1	5.0
$R_S$ (ohms)	1.76	0.48	0.5	1.96
$X_S$ (ohms)	could	4.0	11	33
$L_S$ (microhenries)	not be resolved	2.3	1.7	1.05

(c) Other capacitors + CD bus bar.

Unit	4 mfd., VQ #40		50 mfd., Fast	1 mfd. Mica	50 mfd. VQ 25, 42, and 43
Frequency (mc)	1.1	5.0	1.1	5.0	5.0
$R_S$ (ohms)	0.84	0.67	1.02	0.54	0.65
$L_S$ (microhenries)	0.56	0.82	0.64	0.82	0.82

EVALUATION, CONCLUSIONS

46. The CD apparatus assembled for the HERO studies on the Squib Mk 1 is evaluated as follows:

- (a) Stored energy is known to better than  $\pm 0.5\%$ .
- (b) Ergmeter error in observation of delivered energy (not corrected for diode errors) is  $\pm 1.5\%$ .
- (c) Delivered energy (assuming  $D_{\infty}$  model, equation (3), page 20) is known to better than  $\pm 2\%$ .
- (d) Effect on Squib Mk 1 sensitivity from wave form distortion due to distributed inductance is negligible.
- (e) Errors due to capacitor dielectric leakage are negligible.
- (f) Wave form distortion (prolongation of discharge time constant due to dielectric absorption) is negligible.
- (g) Instrumentation aberration rate, since all suspect data were discarded, assumed to be undetectable.

47. To those who wish to undertake the business of CD sensitivity measurement the use of some form of ergmeter and the use of 100% CRO monitoring is recommended highly. The ergmeter technique most suitable for the particular application may be the bolometer device described herein, some variant of it, or perhaps one depending on the transducer action of a vacuum thermocouple. The best possible CD apparatus would not be expected to give better than 80 to 85% transfer into a 1-ohm load. Efficiencies less than 60% would not be surprising for a "cobbled-up" apparatus. Deterioration and break-down of components can be expected during extended use of an assembly. For any reasonable accuracy of results, then, the ergmeter should be used as a periodic method of checking the quality of the instrumentation. Cathode ray oscillography permits the detection of random (intermittent) malfunctions which could otherwise give rise to serious bias in go-no go testing.

## APPENDIX I

Estimation of Firing System Reliability Requirement

## Assumption

- (1) System Reliability = R  
 (System Failure Rate: F = 1-R)

The probabilities of the various possible results of N trials can be computed from the binominal relationship:

$$(R + F)^N = R^N + NR^{N-1} \cdot F + \frac{N(N-1)R^{N-2} \cdot F^2}{2!} + \dots$$

where  $R^N$  is the probability of no failures,  
 $NR^{N-1} \cdot F$  is the probability of exactly one failure, and  
 $\frac{N(N-1)R^{N-2} \cdot F^2}{2!}$  is the probability of exactly two failures.

Since the likelihood of all fires =  $R^N$ , the likelihood of one or more failures =  $1-R^N$ .

If, with a population of perfect EEDs fired by a switch reliability of R in a large number of N-length runs, a failure is observed in no more than 1 in every 20 runs then the switch reliability must be  $R^N \geq 0.95$ . There would be a 5% chance that malfunction of such a switch used on real initiators would give rise to one or more failures in an N-length run.

Therefore, at 95% confidence, the required system reliability limit,  $R_L$ , as a function of the number of shots is given by:

$$R_L^N = 0.95.$$

As a first approximation:

$$R_L^N = (1-F)^N = 1-NF = 1-N(1-R)$$

or

$$N(1-R_L) = 0.05$$

$$R_L = 1 - \frac{0.05}{N}.$$

Thus, for the Bartlett level where 2 failures were observed 2,486 trials, the firing system failure rate must be 1 in ~ 50,000 or less in order to say that the failures were a property of the squib and not of the system.

APPENDIX II

PRINCIPLES OF THE BOLOMETER-ERGMETER

1. Concept. This instrument is a device to measure the energy content of an electrical pulse. The heart of this instrument is the bolometer. A bolometer is a device of relatively low heat capacity whose resistance is a function of temperature. If the bolometer is made to absorb a burst of energy in a time which is short compared to its inherent cooling time, the bolometer temperature should increase in proportion to the energy absorbed. Since the resistance change should be in proportion to the temperature change, it follows that the change in bolometer resistance should be proportional to the energy dissipated adiabatically in the bolometer. To measure the energy content of an electrical pulse it is necessary to dissipate that pulse (or some known fraction of it) in the bolometer allowing the bolometer to bring about the conversion from electrical to thermal energy. The sensitivity of a bolometer to the energy content of a pulse is inversely proportional to its heat capacity.

2. Design. The Brunswick Instrument Company Model 150 Ergmeter uses a type KP85 bolometer -- 0.3-mil diameter tungsten wire, 100 mils long mounted in an evacuated glass envelope. The resistance is slightly under 5 ohms. The thermal time constant is 0.025 seconds.

In order to utilize the bolometer's properties it is necessary to measure its resistance by passing an electric (polarizing) current through it. By using the bolometer as one arm of a Wheatstone Bridge Circuit, it is possible to arrange the circuitry so that neither (1) the voltage drop across the bolometer due to the polarizing current, nor (2) the transient pulse, will occur at the signal pick-off points A and B of Figure II-1.

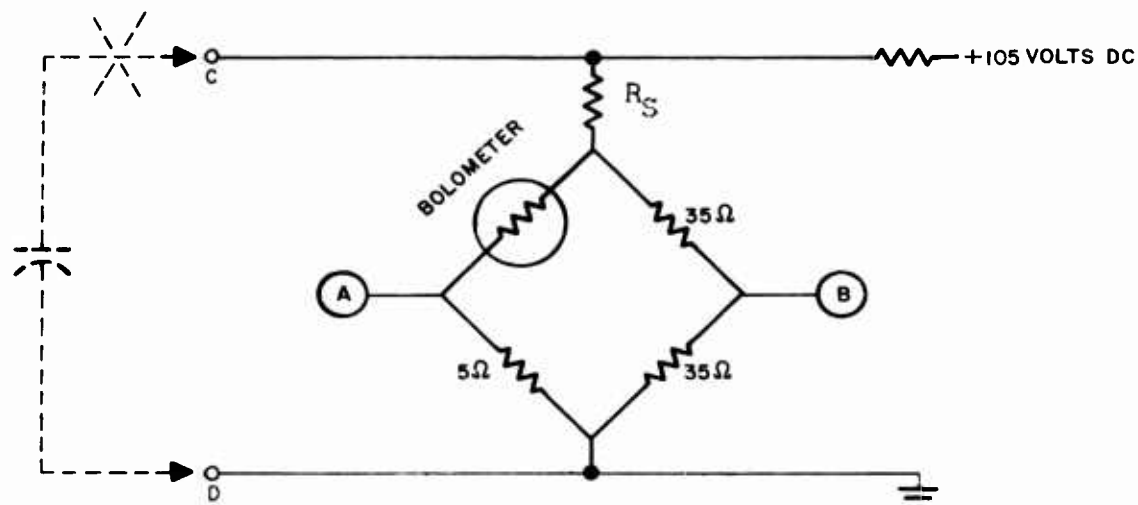


FIG. II-1 BOLOMETER-WHEATSTONE BRIDGE

The magnitude of the polarizing current and the resistance values of the other three bridge arms are adjusted to bring the potential difference between A and B to zero when the system is in the zero condition. Changes in instrument ambient temperature will change the bolometer resistance and therefore the polarizing current to achieve null between A and B unless the bolometer is kept in a temperature-regulated environment such as a crystal oven. Changes in bridge voltage (polarizing current) are to be avoided since they affect system sensitivity.

4. The transient unbalance of the bolometer has a wave-shape such as is shown in Figure II-2 wherein a steeply rising leading edge represents the integration of the energy pulse and the falling portion represents the exponential cooling of the bolometer. The time scales in the diagram have been distorted in order to allow resolution of the rising portion of the transient. By keeping the discharge pulse time less than 1% of the time constant, the system can be considered adiabatic (ballistic) with an error of no more than 1%. The peak amplitude of the transient potential difference between A and B is at most 2 millivolts. In order to be able to measure this transient further instrumentation is needed, in the form of an amplifier driving a voltmeter. Figure II-3 is a symbolic presentation of the chain of elements upon which the ergometer sensing depends.

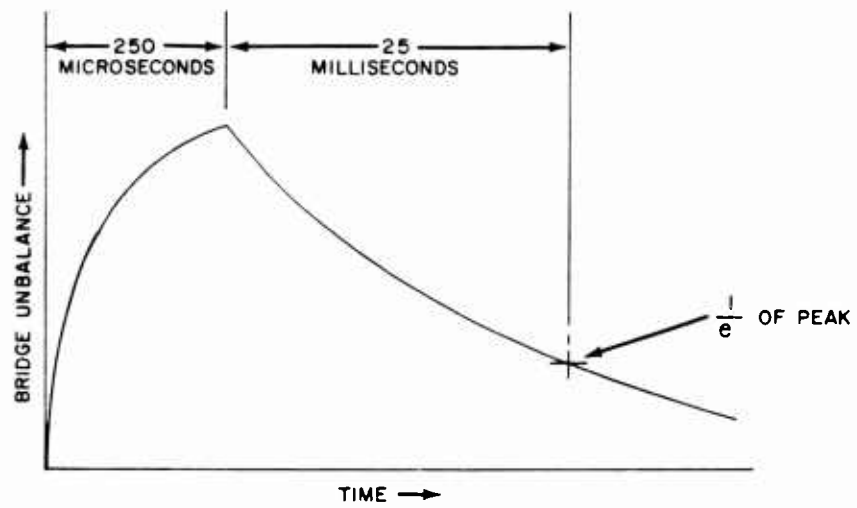


FIG. II-2 BOLOMETER TIME-TEMPERATURE EXCURSION

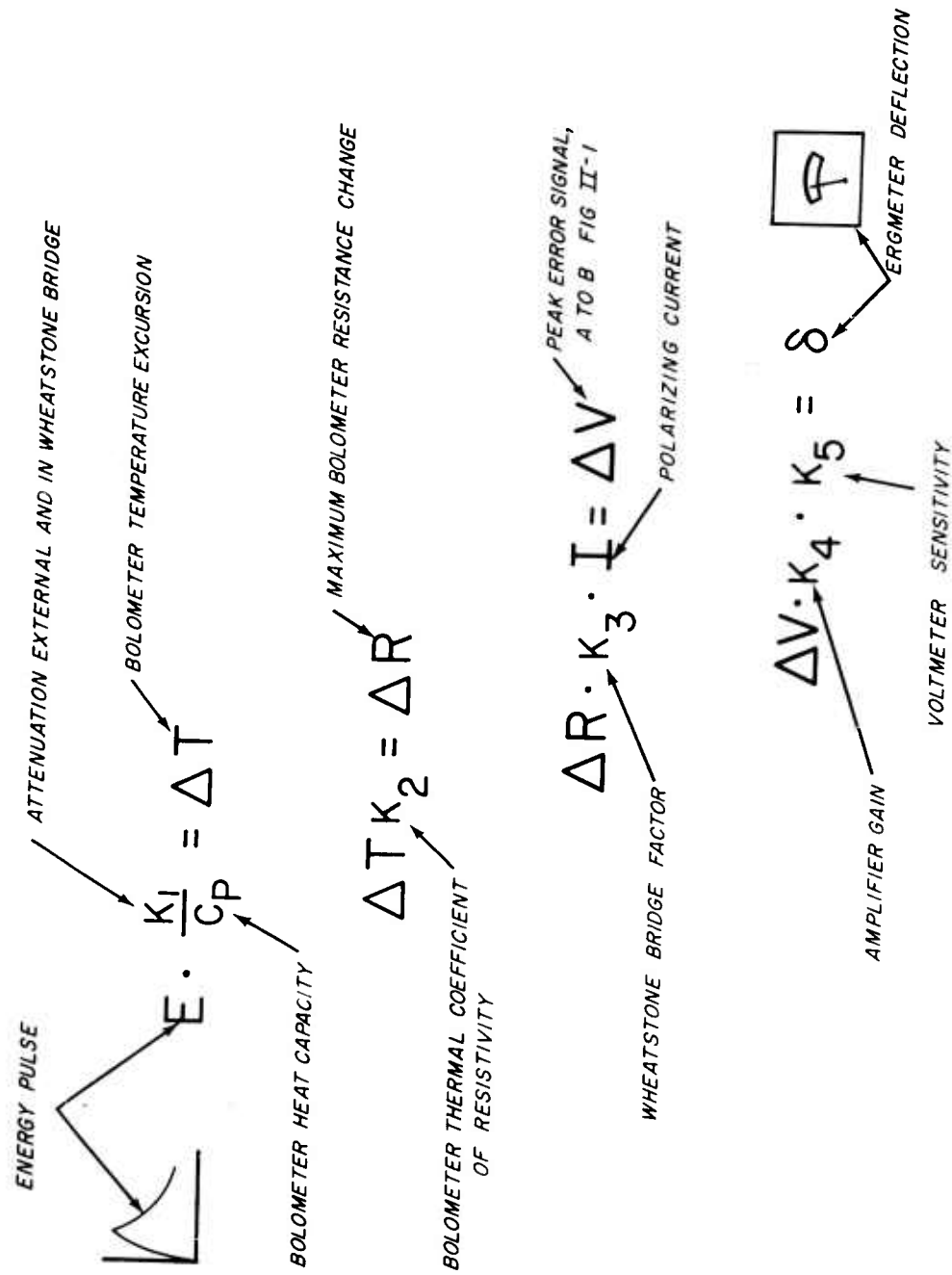


FIG. II-3 SYMBOLIC REPRESENTATION OF ERGMETER

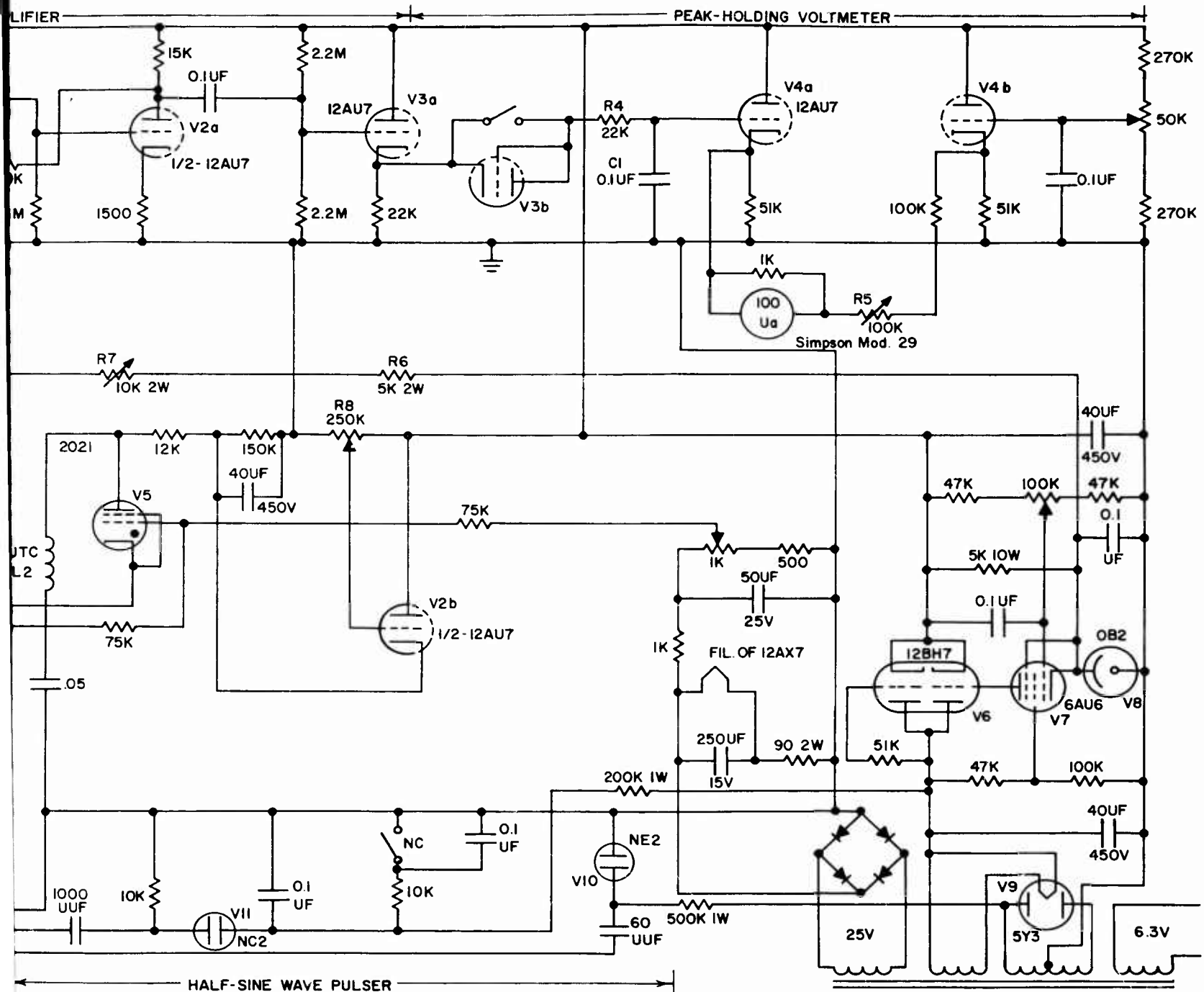
5. In order to ease the ergometer design requirements and simplify its construction and use, it was decided to include a calibration system rather than control, with extreme precision, each of the variables in the previously mentioned chain. For this purpose a half-sine wave pulser\* is included as a part of the Brunswick Model 150 Ergometer. The pulser can be operated either single shot, or repetitively at 60 burst per second, without change in pulse amplitude or form. A vacuum thermocouple (driving an indicating meter) is included as a comparison standard, and is used in the following manner:

- (a) Externally measured DC power is injected into the vacuum thermocouple meter giving a power vs. deflection calibration.
- (b) Half-sine wave pulses at 60 cps are injected. The observed meter deflection gives the DC equivalent power of the train (units in watts, or  $\frac{\text{watt seconds}}{\text{second}}$  or  $\frac{\text{joules}}{\text{second}}$ ).
- (c) One sixtieth of the energy delivered in one second must be the energy of a single burst. This known energy burst, then, can be delivered quantitatively into the bolometer-transducer at an appropriate time. By controlled variations of the half-sine pulse amplitude it is possible to calibrate the ergometer peak holding voltmeter indicator as a function of input energy.

6. Figure II-4 is a diagram of the ergometer. Resistance  $R_5$  is used to trim the bridge (bolometer,  $R_1$ ,  $R_2$ , and  $R_3$ ) to a standard resistance value so that input attenuators will perform as designed. The bolometer bridge "polarizing" current is controlled by  $R_6$  and  $R_7$ . The negative feedback stabilized amplifier ( $V_{1a}$ ,  $V_{1b}$ ,  $B_{2b}$ ,  $V_{3a}$ ) has a gain of about 20,000 and a cathode follower output to drive the diode peak-holding circuit ( $V_{3b}$ ,  $R_4$ ,  $C_1$ ). The diode circuit charging time constant,  $R_4 \cdot C_1$ , is made long enough

\* Electronics, September 1956, "Energy Source Delivers Half-Sine Pulses", by Louis A. Rosenthal.





2

117V 60~ FREED #19123

(2 milliseconds) to suppress response to firing signals that "get past"\* the bolometer bridge. The overall sensitivity of the ergmeter is controlled not by changing the amplifier gain, but rather by controlling the sensitivity of the bridge-type voltmeter (V4a, V4b) by the rheostat R5. The half-sine wave pulse amplitude is controlled by R8.

7. Due to practical limitations in components the ergmeter system is somewhat less than ideal. If these limitations are recognized and compensated for, precision capabilities of the ergmeter are considerably enhanced.

8. Turnover Error. Because of the polarizing current flowing through the bolometer Wheatstone Bridge, there exists a steady-state potential difference across the input terminals. For any capacitor discharge into the input terminals, the potential across the capacitor will swing from the initial voltage,  $V_0$ , to the ergmeter input polarizing voltage,  $V_p$ , rather than from  $V_0$  to complete discharge. The stored energy computation should be given by

$$E_S = \frac{1}{2} C [V_0 - V_p]^2$$

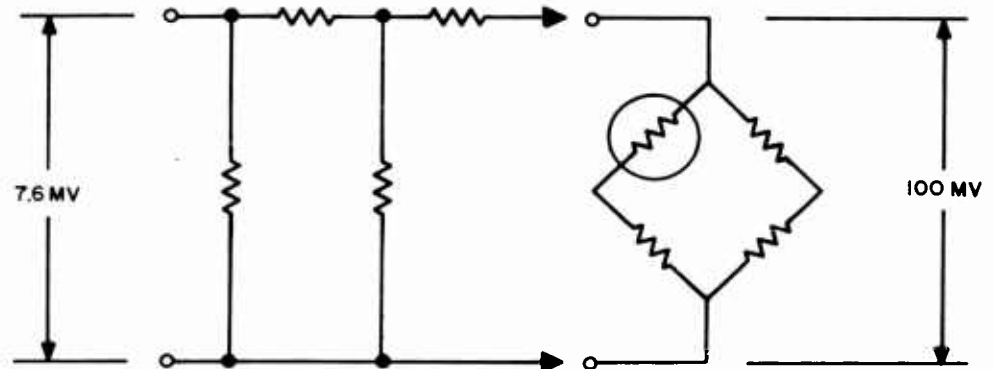
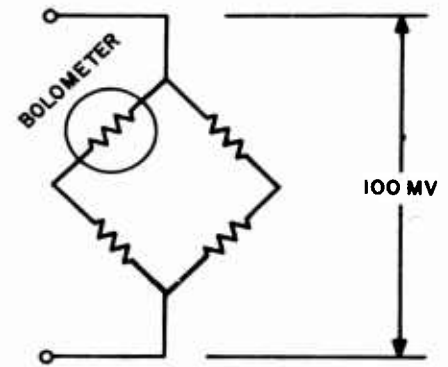
If  $V_p \leq 0.005 V_0$ ,  $V_p$  can be ignored with an error no greater than 1%. This particular effect has been termed "turn-over error" because it can be detected by the difference in ergmeter deflection that would be expected between capacitor discharge into (1) the ergmeter terminals in standard orientation and (2) the ergmeter terminals reversed. For three input arrangements used in the Squib Mk 1 program, Figure II-5 illustrates the magnitude of polarizing potential based on a bridge potential of 100 millivolts. It can be seen that when the ergmeter is used with the 100/1 attenuators, the turnover error can be ignored for charge potentials above 1 volt.

9. Pulse Length Error. As has been mentioned previously the ergmeter will give erroneous indications if the pulse duration is so long that the bolometer is no longer being

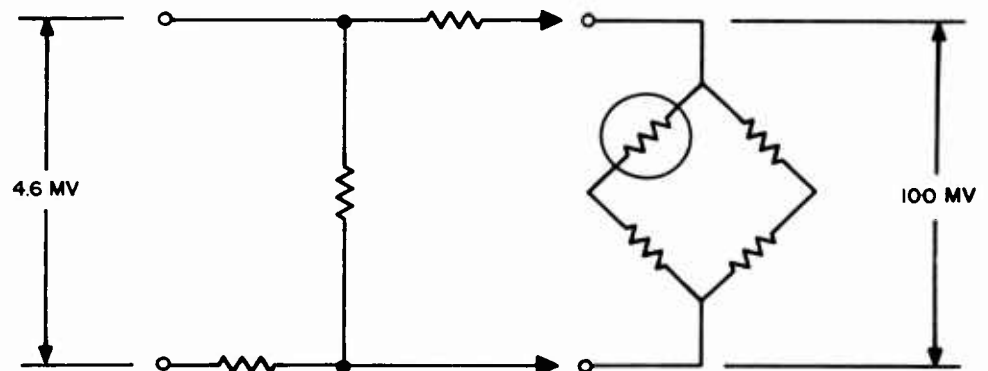
-----

\* It should be remembered that as soon as the bolometer is heated above its ambient temperature by the energy pulse, the bolometer bridge circuit is no longer balanced. Only when the bridge is balanced can it be hoped that none of the firing signal will be fed into the bolometer amplifier.

II-5-a  
NO ATTENUATOR



II-5-b 100/1 LADDER ATTENUATOR, 10Ω INPUT



II-5-c 100/1 LINEAR ATTENUATOR, 1Ω INPUT

FIG. II-5 ERGMETER POLARIZING POTENTIALS

heated adiabatically. This alone sets the maximum pulse length at 250 microseconds for 1% accuracy. The effect of bridge unbalance is less easy to compute. The instantaneous unbalance signal depends upon the instantaneous unbalance of the bridge (which is derived from the integrated energy delivered to it) and the instantaneous amplitude of the input pulse (which depends on the amount of energy remaining in the firing capacitor). The effect of the unbalance signal depends in turn on the "time constant" and amplitude of the unbalance signal compared to the diode integrating network time constant and the voltmeter sensitivity. Since the integrating network time constant is about 2 milliseconds, discharge pulse times much in excess of 20 to 50 microseconds would begin to be suspect. This particular error can be detected as a turn-over error (II - paragraph 8) which is not found with short time constant pulses but does become significant as the pulse length is increased. It is suspected that the maximum time constant that could be tolerated would depend upon the potential on the capacitor. That is, even though the time constant were somewhat long the effect would be less serious when the peak voltage seen at the bridge input terminals is less. This concept is expressed symbolically below:

$$e = \frac{R \cdot C \cdot V_0}{R_4 \cdot C_1 \cdot V_B}$$

where  $e$  = unbalance error

$R$  = attenuator (or ergmeter) input resistance

$C$  = firing capacity

$V_0$  = charge potential

$R_4 \cdot C_1$  = integration time constant

$V_B$  = bolometer bridge polarizing potential.

10. Diode Errors. Two types of error due to the limitation of practical diodes must be considered. Because there must be some potential difference between the anode and cathode of a vacuum-tube diode the diode will appear to have a certain "backlash" or "dead zone" where conduction does not take place even though the anode is more positive than the cathode. This potential displacement, known as contact potential, will censor the bottom edge of the signal (see Figure II-6) applied to the diode storage capacitor and will lead to an undercharge of the capacitor and hence an underestimate of the true delivered energy.

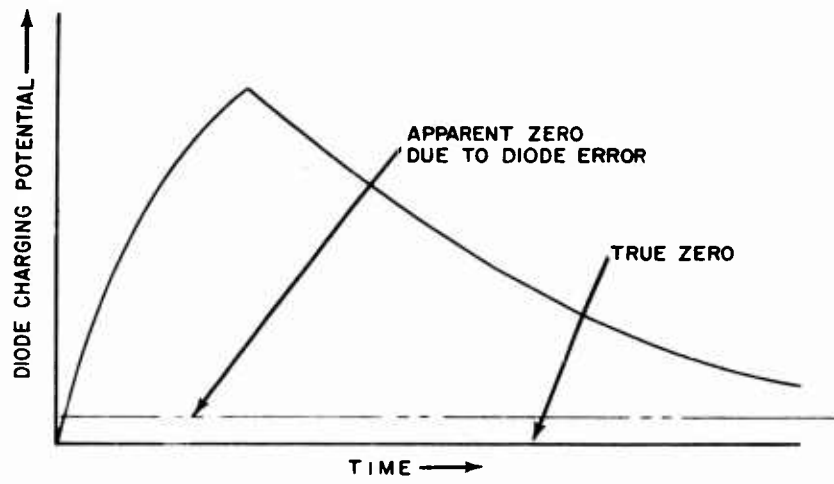


FIG. II-6 CONTACT POTENTIAL DIODE ERROR

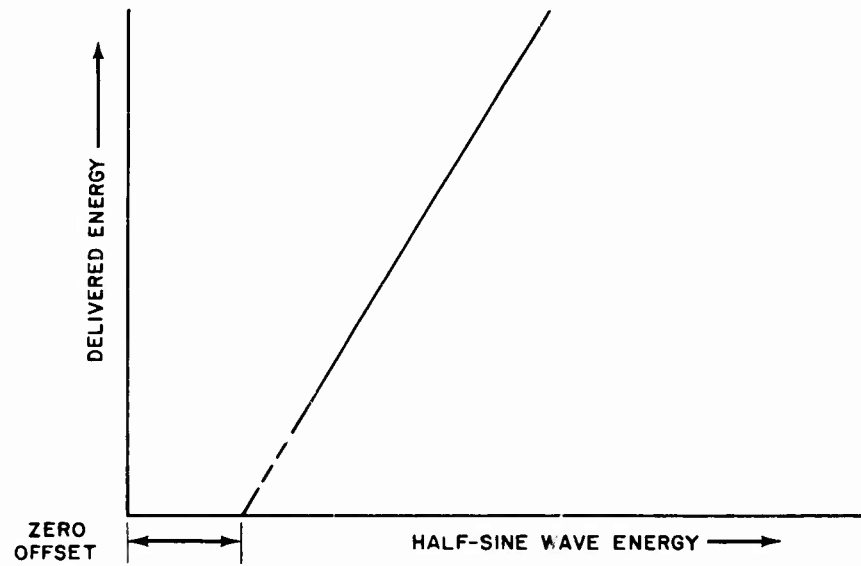


FIG. II-7 TOTAL DIODE ERROR

11. Another type of limitation in the diode is that when the anode-cathode potential difference is slightly greater than the contact potential, the forward resistance of the diode is considerably greater than is the case for larger potential differences. As a consequence, as the transient from the bolometer amplifier reverts to balance conditions after the main pulse has been fed to the storage capacitor, the diode charging time constant begins to rise and less than the true amount of charge is conveyed to the capacitor. Both forms of diode deviations combine to give the same type of ergmeter error. The error becomes proportionally larger for smaller total voltage excursions of the storage capacitor. The magnitude of the total diode error can be found by plotting delivered energy versus half-sine wave burst energy for a given setting of bolometer bridge polarizing current and a given voltmeter sensitivity. A straight line should be observed, as in Figure II-7, with a "zero-offset" indicating a level below which energy can be delivered to the ergmeter without any observable response. The portion of the "zero-offset" due to contact potential can be found by injecting DC potentials ahead of the cathode follower, V3a, and by making a similar plot of response versus DC input potential.

## NavWeps Report 7308

## DISTRIBUTION

	Copies
Director of Defense Research & Development Department of Defense Washington 25, D. C.	1
Chief of Naval Operations (OP 411H) Department of Navy Washington 25, D. C.	1
Chief, Bureau of Naval Weapons Department of Navy Washington 25, D. C.	
DLI-32	2
RRRE-8	1
RUME-3	1
RUME-32	1
RMMO-2	1
RMMP-3	1
RMMO-4	1
RREN-312	1
Director Special Projects Office Washington 25, D. C.	
SP-20	4
SP 27	1
Chief, Bureau of Ships Department of Navy Washington 25, D. C. Code 423	2
Chief, Bureau of Yards & Docks Department of Navy Washington 25, D. C. Code D-200	1
Chief of Naval Research Department of Navy Washington 25, D. C. Chemistry Branch	2
Commandant U. S. Marine Corps Washington 25, D. C.	1

NavWeps Report 7308

Commander Operational Development Force U. S. Atlantic Fleet U. S. Naval Base Norfolk 11, Virginia	2
Commander U. S. Naval Ordnance Test Station China Lake, California Code 556 Code 4572 Technical Library B. A. Breslow J. Sherman	1 1 1 2 1 1
Director Naval Research Laboratory Washington 25, D. C. Technical Information Section	2
Director David Taylor Model Basin Carderock, Maryland Dr. A. H. Keil	2
Commander Naval Air Development Center Johnsville, Pennsylvania Aviation Armament Laboratory	1
Commander U. S. Naval Weapons Laboratory Dahlgren, Virginia Technical Library J. Payne (WH Div.)	2 1
Commander U. S. Naval Air Test Center Patuxent River, Maryland	1
Commander Naval Air Missile Test Center Point Mugo California	1
Commanding Officer U. S. Naval Weapons Station Yorktown, Virginia R & D Division	2

NavWeps Report 7308

Commanding Officer U. S. Naval Ordnance Laboratory Corona, California	2
Commanding Officer U. S. Naval Propellant Plant Indian Head, Maryland Technical Library EODTC	1 1
Commander Naval Radiological Defense Laboratory San Francisco, California	1
Commander U. S. Naval Weapons Plant Washington 25, D. C.	1
Commanding Officer U. S. Naval Ordnance Plant Macon, Georgia	1
Commanding Officer U. S. Naval Ammunition Depot McAlester, Oklahoma R. E. Halpern	1
Commanding Officer U. S. Naval Ammunition Depot Waipale Branch Oahu, Hawaii Special Projects Officer Quality Evaluation Laboratory	1
Commanding Officer U. S. Naval Ammunition Depot Navy Number Six Six (66) c/o Fleet Post Office San Francisco, California	1
Commanding Officer U. S. Naval Ammunition Depot Bangor, Maine Quality Evaluation Laboratory	1
Commanding Officer U. S. Naval Ammunition Depot Concord, California Quality Evaluation Laboratory	1

NavWeps Report 7308

Commanding Officer U. S. Navy Electronics Laboratory San Diego 52, California	1
Commanding Officer U. S. Naval Underwater Ordnance Station Newport, Rhode Island	1
Commanding Officer U. S. Naval Air Special Weapons Facility Kirtland Air Force Base Albuquerque, New Mexico	1
Commanding Officer U. S. Naval Nuclear Ordnance Evaluation Unit Albuquerque, New Mexico	1
Commanding Officer Naval Torpedo Station Keyport, Washington	1
Office of Chief of Ordnance Department of Army Washington 25, D. C.	
ORDGU	1
ORDTN	1
ORDTB	1
Office of Chief Signal Officer Research & Development Division Washington 25, D. C.	1
Office of Chief of Engineers Department of Army Washington 25, D. C.	
ENGNB	1
ENGEB	1
Commanding General Picatinny Arsenal Dover, New Jersey	
ORDBB-TH8	1
ORDBB-TJ1	1
ORDBB-TK3	1
ORDBB-TM1	1
ORDBB-TP1	1
ORDBB-TP2	1
ORDBB-TP3	1
ORDBB-TR2	1
ORDBB-TS1	1

NavWeps Report 7308

Commanding Officer Army Signal Research & Development Laboratory Fort Monmouth, New Jersey	1
Commanding Officer Office of Ordnance Research Duke Station Durham, North Carolina	1
Commander U. S. Army Ordnance Frankford Arsenal Philadelphia 37, Pa.	1
Commander U. S. Army Rocket & Guided Missile Agency Redstone Arsenal, Alabama	1
Commanding Officer Diamond Ordnance Fuze Laboratory Connecticut Avenue & Van Ness St., N. W. Washington 25, D. C.	
Ordnance Development Laboratory	1
M. Lipnick (Code 005)	1
R. Comyn (Code 710)	1
George Keehn (Code 320)	1
Chief of Staff U. S. Air Force Washington 25, D. C. AFORD-AR	1
Commander Wright Air Development Center Wright-Patterson Air Force Base Dayton, Ohio	1
Commander Air Material Armament Test Center Eglin Air Force Base, Florida	1
Commander Air Research & Development Command Andrews Air Force Base Washington 25, D. C.	1
Commander Rome Air Development Center Griffiss Air Force Base Rome, New York	1

NavWeps Report 7308

Commander Holloman Air Development Center Alamogordo, New Mexico	1
Commanding Officer Air Force Missile Test Center Patrick Air Force Base Florida	1
Commander Air Force Cambridge Research Center L. G. Hanscom Field Bedford, Massachusetts	1
Commander OOAMA Hill Air Force Base Utah	1
Armed Services Technical Information Agency Arlington Hall Station Arlington, Virginia TIPDR	10
Office of Technical Services Department of Commerce Washington 25, D. C.	100
Director U. S. Bureau of Mines Division of Explosive Technology 4800 Forbes Street Pittsburgh 13, Pennsylvania	1
Atomic Energy Commission Washington 25, D. C. DMA	1
Lawrence Radiation Laboratory University of California P. O. Box 808 Livermore, California Technical Information Division	1
Director Los Alamos Scientific Laboratory P. O. Box 1663 Los Alamos, New Mexico Library	1

NavWeps Report 7308

Stavid Engineering Inc. U. S. Route 22 Plainfield, New Jersey	1
Vitro Corporation 14000 Georgia Avenue Silver Spring, Maryland	1
Western Cartridge Company Division of Olin Industries East Aiton, Illinois	1
Denver Research Institute University of Denver Denver 10, Colorado	1
Universal Match Corporation Ordill, Illinois Mr. Wm. Rose	1
Universal Match Corporation Marion, Illinois	1
Bermite Powder Company Saugus, California	1
Field Command, Defense Atomic Support Agency Albuquerque, New Mexico (attn:FCDR)	1
Defense Atomic Support Agency Washington 25, D. C.	2